



**HAL**  
open science

# Why the Ala-His-His Peptide Is an Appropriate Scaffold to Remove and Redox Silence Copper Ions from the Alzheimer's-Related A $\beta$ Peptide

Paulina Gonzalez, Laurent Sabater, Emilie Mathieu, Peter Faller, Christelle Hureau

## ► To cite this version:

Paulina Gonzalez, Laurent Sabater, Emilie Mathieu, Peter Faller, Christelle Hureau. Why the Ala-His-His Peptide Is an Appropriate Scaffold to Remove and Redox Silence Copper Ions from the Alzheimer's-Related A $\beta$  Peptide. *Biomolecules*, 2022, 12 (10), pp.1327. 10.3390/biom12101327 . hal-03799992

**HAL Id: hal-03799992**

**<https://hal.science/hal-03799992v1>**

Submitted on 6 Oct 2022

**HAL** is a multi-disciplinary open access archive for the deposit and dissemination of scientific research documents, whether they are published or not. The documents may come from teaching and research institutions in France or abroad, or from public or private research centers.

L'archive ouverte pluridisciplinaire **HAL**, est destinée au dépôt et à la diffusion de documents scientifiques de niveau recherche, publiés ou non, émanant des établissements d'enseignement et de recherche français ou étrangers, des laboratoires publics ou privés.



Distributed under a Creative Commons Attribution 4.0 International License

## Article

# Why the Ala-His-His Peptide Is an Appropriate Scaffold to Remove and Redox Silence Copper Ions from the Alzheimer's-Related A $\beta$ Peptide

Paulina Gonzalez <sup>1,2</sup> , Laurent Sabater <sup>1</sup>, Emilie Mathieu <sup>1</sup> , Peter Faller <sup>2</sup>  and Christelle Hureau <sup>1,\*</sup><sup>1</sup> LCC-CNRS, Université de Toulouse, CNRS, 31077 Toulouse, France<sup>2</sup> Laboratory of Biometals and Biological Chemistry, Institut de Chimie (UMR 7177), Université de Strasbourg-CNRS, 4 rue Blaise Pascal, 67000 Strasbourg, France

\* Correspondence: christelle.hureau@lcc-toulouse.fr

**Abstract:** The progressive, neurodegenerative Alzheimer's disease (AD) is the most widespread dementia. Due to the ageing of the population and the current lack of molecules able to prevent or stop the disease, AD will be even more impactful for society in the future. AD is a multifactorial disease, and, among other factors, metal ions have been regarded as potential therapeutic targets. This is the case for the redox-competent Cu ions involved in the production of reactive oxygen species (ROS) when bound to the Alzheimer-related A $\beta$  peptide, a process that contributes to the overall oxidative stress and inflammation observed in AD. Here, we made use of peptide ligands to stop the Cu(A $\beta$ )-induced ROS production and we showed why the AHH sequence is fully appropriate, while the two parents, AH and AAH, are not. The AHH peptide keeps its beneficial ability against Cu(A $\beta$ )-induced ROS, even in the presence of Zn<sup>II</sup>-competing ions and other biologically relevant ions. The detailed kinetic mechanism by which AHH could exert its action against Cu(A $\beta$ )-induced ROS is also proposed.

**Keywords:** ATCUN; copper; amyloid- $\beta$ ; peptides; ROS; kinetics; drug candidates



**Citation:** Gonzalez, P.; Sabater, L.; Mathieu, E.; Faller, P.; Hureau, C. Why the Ala-His-His Peptide Is an Appropriate Scaffold to Remove and Redox Silence Copper Ions from the Alzheimer's-Related A $\beta$  Peptide. *Biomolecules* **2022**, *12*, 1327. <https://doi.org/10.3390/biom12101327>

Academic Editor: Anne Kasus-Jacobi

Received: 20 August 2022

Accepted: 13 September 2022

Published: 20 September 2022

**Publisher's Note:** MDPI stays neutral with regard to jurisdictional claims in published maps and institutional affiliations.



**Copyright:** © 2022 by the authors. Licensee MDPI, Basel, Switzerland. This article is an open access article distributed under the terms and conditions of the Creative Commons Attribution (CC BY) license (<https://creativecommons.org/licenses/by/4.0/>).

## 1. Introduction

Alzheimer's disease (AD) is a progressive, neurodegenerative disorder affecting neurons in specific places in the brain, causing cognitive impairment and disability in daily life activities. It represents more than half of all dementia cases, which are listed as the world's seventh leading cause of death [1–5]. The number of patients suffering from dementia is 55 million, a number that will dramatically increase in the near future (a double-to-triple increase is expected on the horizon of 2050). This is due, first, to the ageing of the population, but also to the lack of disease-modifying drugs, *id est*, molecules able not only to relieve symptoms, but also to intervene in the neurodegenerative process.

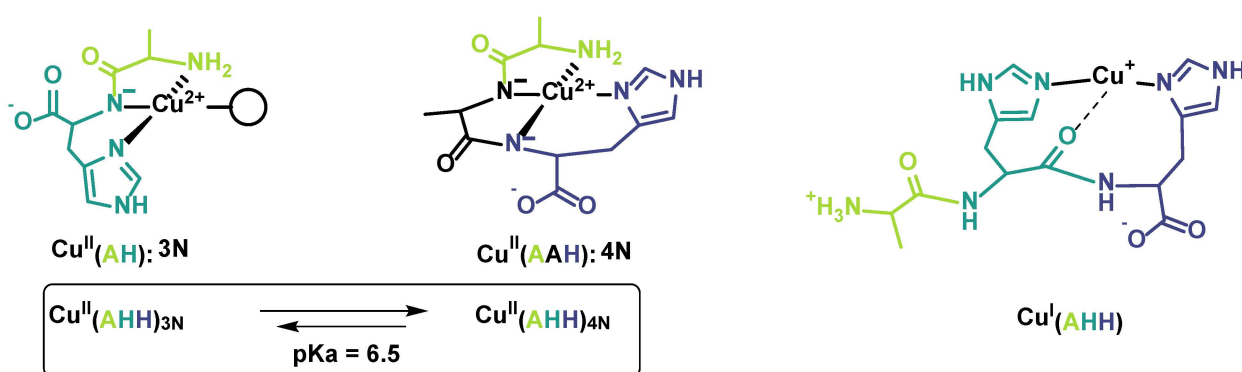
AD is multifactorial and several therapeutic targets are currently being investigated [6–9]. This is the case for instance of the amyloid- $\beta$  (A $\beta$ ) peptide [5,10] and the hyperphosphorylated Tau protein [11,12] that can assemble to form extracellular amyloid deposits and intracellular tangles, respectively. In the present article, we focus on the redox-competent copper (Cu) ions [13–18]. Cu ions have been shown to modify the assembly properties of A $\beta$  [19]. Beyond that, Cu ions have the ability to generate Reactive Oxygen Species (ROS) when bound to A $\beta$  that contribute to the overall oxidative stress observed in AD in relation with neuro-inflammation [20,21]. Cu(A $\beta$ )-catalyzed incomplete reduction of dioxygen fueled by biological reductants such as ascorbate (Asc) leading to superoxide, [22] hydrogen peroxide [23] and hydroxyl radicals [24,25] have been reported. As a direct consequence, we and others have developed therapeutic approaches targeting Cu ions with the aim to extract them from A $\beta$  and to redox silence them [13–17].

Here, we make use of a short peptide, namely the Ala-His-His-COOH (AHH), to illustrate why such peptide scaffolds are highly suitable to stop the production of ROS induced by Cu(A $\beta$ ). The main drawback of peptides, *id est*, a weak proteolytic stability [26], is currently the subject of intense lines of research aimed at overcoming such issues, either by the use of peptidomimetic molecules [27–29], D-isomers, [30] or smart delivery systems [31–34]. In contrast, peptides have the great advantage of being easily tunable. For instance, cell-penetrating peptides (CPP) [35], including brain-penetrating sequences [36], could easily be appended to improve blood–brain barrier entrance. Another possibility would be the combination with peptide-based scaffolds built on poly(His) [37] and poly(Glu) [38] and recently reported as drug delivery vehicles. Hence, peptides are fully appropriate drug candidates.

A key point to consider is the Cu versus Zn selectivity of the intended peptide sequences. Indeed Zn<sup>II</sup> is present in the synaptic cleft at concentrations much higher (about 10 to 100-fold) than Cu and can thus interfere with Cu detoxification [39]. Both ions have been reported to bind to the N-terminal part of the A $\beta$  peptide (having the sequence DAEFRGHDSGYEVHHQK, *id est*, H<sub>2</sub>N-Asp-Ala-Glu-Phe-Arg-His-Asp-Ser-Gly-Tyr-Glu-Cal-His-His-Gln-Lys-COOH, see Scheme S1, named A $\beta$ <sub>1–16</sub>, where the full-length peptides are 40- and 42-amino-acids-long: A $\beta$ <sub>1–40/42</sub>, here, A $\beta$ <sub>1–16</sub>, is noted A $\beta$ , but with distinct binding sites [39–41]. At neutral pH, Cu<sup>II</sup> is bound to the terminal amine, two imidazole rings from two of the three His at positions 6, 13, and 14, and the peptide carbonyl function of Asp1-Ala2, [42] while Zn<sup>II</sup> is bound by two imidazole rings from the His and two carboxylate (from Asp1, Glu3, Asp7, or Glu11) [43] and Cu<sup>I</sup> by two imidazole rings from the His [44,45]. The A $\beta$  affinity of Cu<sup>II</sup> is about 10<sup>9</sup> M<sup>−1</sup> [46] that of Zn<sup>II</sup> 10<sup>5</sup> M<sup>−1</sup> [47], while for Cu<sup>I</sup>, this is still under debate, with values ranging from 10<sup>6</sup> to 10<sup>10</sup> M<sup>−1</sup> [48–50]. Hence, the Cu over Zn selectivity of the intended peptide ligand should overcome that of A $\beta$ , that is, 10<sup>4</sup> in case of Cu<sup>II</sup>.

Cu<sup>II</sup> binding to the short AHH peptide was previously studied using a set of spectroscopy and it was shown that it has the ability to bind Cu<sup>II</sup> in two different sites at neutral pH (Scheme 1) [51]. The AHH peptide is issued from AH and AAH that were also studied here for comparison purposes. AH is a canonical Cu<sup>II</sup>-binding motif found in the wound-healing factor GHK peptide involved in anti-inflammation process [52–54] and binds to Cu<sup>II</sup> via the terminal amine, the His imidazole ring, and the deprotonated amide in between, thus leaving a labile site on the fourth equatorial position (Scheme 1, 3N coordination mode) [55]. AAH contains the ATCUN (Amino-Terminal CU and Ni-binding) motif, which, by definition, has one histidine in the third position and a free terminal amine [56–59]. In ATCUN peptides, Cu<sup>II</sup> is bound by the terminal amine, the His imidazole ring, and the two deprotonated amides in between (Scheme 1, 4N coordination mode) [55]. In AHH, having His at both positions 2 and 3, the switch between the 3N and 4N motifs can be driven by pH [51] and by the addition of external ligands such as imidazole, in the presence of which the Cu<sup>II</sup> complexes equilibrated between 4N and a 3N + 1N coordination mode [60]. The three peptides may fulfill the selectivity criteria, since Cu<sup>II</sup> affinity lies in the 10<sup>12</sup>–10<sup>14</sup> M<sup>−1</sup> range for such motifs [56–59,61,62], while Zn<sup>II</sup> affinity is expected to be weaker than the one of A $\beta$ . Indeed, there are fewer than three Zn<sup>II</sup> binding atoms in the peptides, since Zn<sup>II</sup> is not able to induce the deprotonation of the peptide bond in contrast to Cu<sup>II</sup>, which is the event leading to the huge affinity observed in the case of Cu<sup>II</sup> [63,64].

In the present article, we report on the ability of the chimera peptide AHH to stop Cu(A $\beta$ )-produced ROS using the ascorbate consumption assay as a leading method, and we tentatively propose a mechanism of action. ATCUN peptides and their derivatives have been used in several biomedical applications [65,66], including against AD [67–73]. The added value of the AHH peptide is discussed later in the text.



**Scheme 1.**  $\text{Cu}^{\text{II}}$ -binding sites in AH, AAH at neutral pH, and pH-dependent equilibrium of  $\text{Cu}(\text{AHH})$ .  $\text{Cu}^{\text{I}}$ -binding site in AHH (proposed based on literature data, the participation of the  $-\text{CO}$  from the peptide bond is still under debate) [48–50,74,75].

## 2. Results and Discussion

### 2.1. Effect on $\text{Cu}$ - and $\text{Cu}(\text{A}\beta)$ -Induced ROS Production

The effect of AH, AAH, and AHH on the  $\text{Cu}$ - and  $\text{Cu}(\text{A}\beta)$ -induced ROS production was investigated by following ascorbate (Asc) consumption by UV–Visible spectroscopy at 265 nm ( $\epsilon_{\text{Asc}} = 14,500 \text{ M}^{-1} \cdot \text{cm}^{-1}$ ) (Figure 1 and Figure S1). It was previously shown that, because Asc fuels the production of ROS, following its consumption is a straightforward way to monitor the formation of ROS production,  $\text{H}_2\text{O}_2$ , or  $\text{HO}^\circ$  [76,77]. Hence, this is a standard and well-accepted method [16], with less bias than other ROS detection assays [78]. Two kinds of experiments were performed: (i) Asc is added once the peptide (AH, AAH, and AHH, noted pep unless specified) has been mixed with  $\text{Cu}^{\text{II}}$  or  $\text{Cu}^{\text{II}}(\text{A}\beta)$  (Figure S1) or (ii) the peptide is added during the course of Asc consumption triggered by  $\text{Cu}^{\text{II}}$  or  $\text{Cu}^{\text{II}}(\text{A}\beta)$  (Figure 1). With the first experiment (Figure S1),  $\text{Cu}^{\text{II}}$  or  $\text{Cu}^{\text{II}}(\text{A}\beta)$  and the peptides are premixed in solution before the addition of Asc to evidence differences in the redox properties of the  $\text{Cu}^{\text{II}}(\text{pep})$  complexes (when added to  $\text{Cu}^{\text{II}}$ ) and the peptide ability to remove  $\text{Cu}^{\text{II}}$  from  $\text{A}\beta$  (when added to  $\text{Cu}^{\text{II}}(\text{A}\beta)$ ). With the second experiment (Figure 1), the kinetics of  $\text{Cu}^{\text{II}}$  complexation are additionally probed; indeed, there is a competition between the reduction of  $\text{Cu}^{\text{II}}$  or  $\text{Cu}^{\text{II}}(\text{A}\beta)$  by Asc and the  $\text{Cu}^{\text{II}}$  uptake by the ligand [79,80].

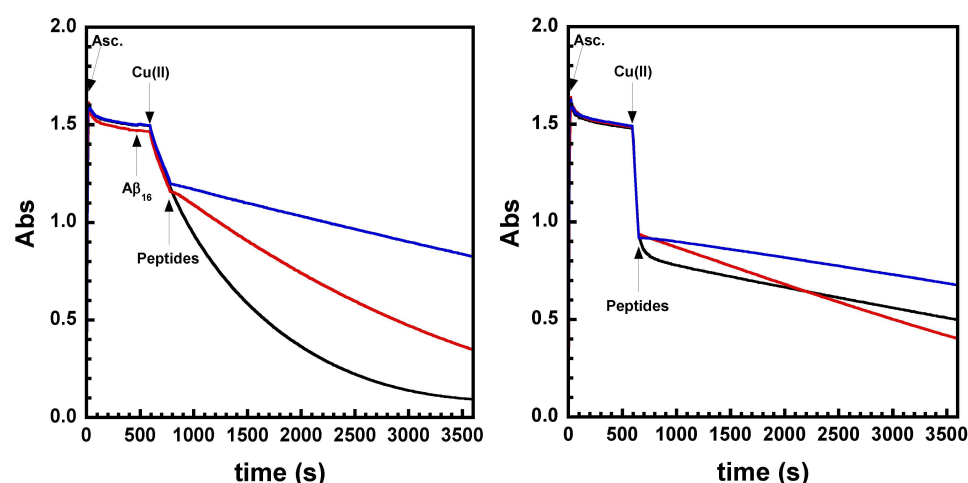


**Figure 1.** Ascorbate consumption (measured at  $\lambda = 265 \text{ nm}$ ) as a function of time. Ascorbate was added first, followed by  $\text{A}\beta_{1-16}$  (right panel) after 6 min, and  $\text{Cu}^{\text{II}}$  after 10 min, and the peptides (AH in red, AAH in black, and AHH in blue) when an absorbance of 1.0 (left) or 1.2 (right) was reached. Measurements were performed in 50 mM HEPES buffer (pH 7.5) at 25 °C with continuous stirring. Final concentrations:  $[\text{Asc}] = 100 \mu\text{M}$ ,  $[\text{A}\beta] = 12 \mu\text{M}$ ,  $[\text{Peptide}] = 12 \mu\text{M}$ ,  $[\text{Cu}^{\text{II}}] = 10 \mu\text{M}$ .

With Cu (in absence of A $\beta$ ), AH displays a steeper slope than AAH and AHH, indicating that AH is not able to stop Cu-induced Asc consumption (Figures 1 and S1, red lines, left). This is in accordance with the ability of AH to bind Cu<sup>II</sup> only in a 3N-motif, the resulting complex Cu(AH) being redox-active [55]. AAH is able to prevent or stop Asc consumption in conditions corresponding to pre-mixture or added during Asc consumption, respectively (Figure 1 and Figure S1, black lines, left). This is in line with the formation of a redox-inert Cu(AAH) complex where Cu<sup>II</sup> is bound in a 4N-motif, which is resistant to reduction by Asc, in line with previously reported electrochemical data [51]. As shown in Figure 1, panel A (between  $t = 600$  and  $700$  s, black curve), the change in the slope to reach a straight line is not immediate (as for AH and AHH) and a delay is thus observed between the addition of AAH and the total slowdown of Cu-induced Asc consumption. This indicates slow kinetics of complex formation. AHH displays the best ability to limit Asc consumption in both experiments (Figures 1 and S1, blue lines, left), which suggests a fast complexation of Cu<sup>II</sup> by the peptide and the subsequent formation of a complex which cannot be reduced by Asc.

The effect of AH, AAH, and AHH was then investigated on Cu(A $\beta$ )-induced ROS production (Figure 1 and Figure S1, right). Similar to the precedent experiments, the ability of AH, AAH, and AHH to limit Asc consumption was tested in pre-mixed (Figure S1, right) or addition during Asc consumption (Figure 1, right) conditions. The results show the ability of AH to remove Cu from A $\beta$  and slow down Asc consumption, but not completely, due to the ability of Cu<sup>II</sup>(AH) to react with Asc, as shown in the experiments without A $\beta$  being present. AAH was able to stop Asc consumption when AAH was first premixed with Cu(A $\beta$ ) (Figure S1, right), but not when it was added during Cu(A $\beta$ )-induced Asc consumption (Figure 1, black lines, right). Since binding of Cu<sup>II</sup> by AAH is thermodynamically favored compared to A $\beta$ , these results indicate that the slow kinetics of Cu<sup>II</sup> extraction from A $\beta$  hampered AAH from efficiently halting related Asc consumption. Finally, AHH was able to lessen Asc consumption efficiently regardless of the conditions (Figure 1 and Figure S1, blue lines, right)). The arrest of ROS production is, however, not total.

To gain further insights into the mechanism by which AHH lessens Cu<sup>II</sup>/Cu<sup>II</sup>(A $\beta$ )-induced Asc consumption, the experiments were performed at different pH, with (Figure 2) and without A $\beta$  (Figure S2). The effect of AHH on Cu and Cu(A $\beta$ )-induced Asc consumption is pH-dependent: the higher the pH is, the better the arrest of ROS production. The pH-dependent ability of AHH to limit Asc consumption reflects the pH-driven switch of AHH between the 3N and 4N-motifs, since this equilibrium has a pK<sub>a</sub> of  $\sim 6.5$ . Hence, at pH 6.8, there is about 30% of the complex Cu(AHH) in a redox-competent 3N-motif, while at pH 8.2, >95% of the formed complex is in the 4N form resistant to Asc reduction.

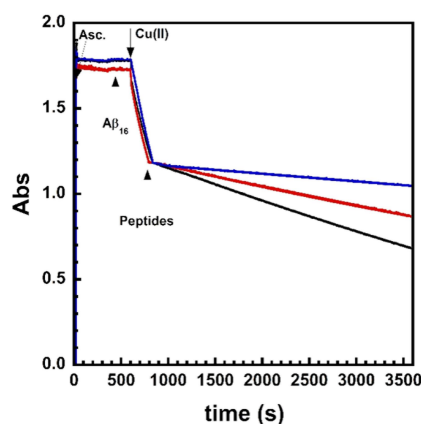


**Figure 2.** Ascorbate consumption (measured at  $\lambda = 265$  nm) as a function of time. Ascorbate was added first, followed by by A $\beta_{1-16}$  after 6 min and Cu<sup>II</sup> after 10 min, and, finally, the AHH peptides at three pH values: 6.8 (black), 7.5 (red), and 8.2 (blue), when an absorbance of 1.2 was reached. Measurements were performed in 50 mM HEPES buffer (pH 7.5) at 25 °C with continuous stirring. Final concentrations: [Asc] = 100  $\mu$ M, [AHH] = 12  $\mu$ M, Cu<sup>II</sup> = 10  $\mu$ M.

At this stage, we can hypothesize that AHH first binds  $\text{Cu}^{\text{II}}$  in a 3N motif, which would induce kinetics similar to that of AH, and then rearranges in a 4N-redox-inactive motif as AAH. According to this hypothesis, the peptide would combine the two positive effects of the 3N and 4N motifs, which are a fast  $\text{Cu}^{\text{II}}$ -binding kinetic, and the formation of a redox-inactive  $\text{Cu}^{\text{II}}$  complex, respectively. To question this hypothesis, we investigated the kinetics of  $\text{Cu}^{\text{II}}$  captured by the peptides by stopped-flow experiments.

## 2.2. Kinetics of Cu and Cu(A $\beta$ ) Capture by the Peptides

First, stop-flow experiments were performed by mixing  $\text{Cu}^{\text{II}}$  with the peptides and recording absorption spectra with an integration time of 1 ms (Figure 3, Figures S3 and S4). The appearance of the Cu(pep) UV-Vis signature was monitored at 530 nm and 590 nm, corresponding, respectively, to the maximum absorption for Cu(AAH) (4N) and Cu(AH) (3N) species [51]. By the naked eye, it can be seen that the rate of Cu(pep) formation is  $\text{Cu}(\text{AH}) > \text{Cu}(\text{AHH}) > \text{Cu}(\text{AAH})$ , in line with the previously described ROS results. Cu(AH) formation is too fast to be measured with this technique and is completed in less than 5 ms, which corresponds to the dead time of the UV-Vis stopped-flow spectrometer. Since several steps are at play (see below), the overall kinetic rates of Cu(AAH) and Cu(AHH) formation were evaluated by the  $t_{1/2}$ , at which half of the final  $\text{Cu}^{\text{II}}$ (pep) complexes are formed at various wavelengths (Table 1). Cu(AHH) formation is about eight times faster ( $t_{1/2} = 18$  ms) than Cu(AAH) formation ( $t_{1/2} = 150$  ms).

**Table 1.** Parameters for the kinetics of formation of  $\text{Cu}^{\text{II}}$ -peptide complex.

Conditions [a]	$t_{1/2}$ [ms]	Corresponding Mainly to
AH + Cu	<5	/
AAH + Cu	$150 \pm 20$	2N to 4N conversion
AHH + Cu	$18 \pm 20$	2N and/or 3N to 4N conversion
AHH + Cu(A $\beta$ )	$250 \pm 50$	Formation of 2N and/or 3N intermediates

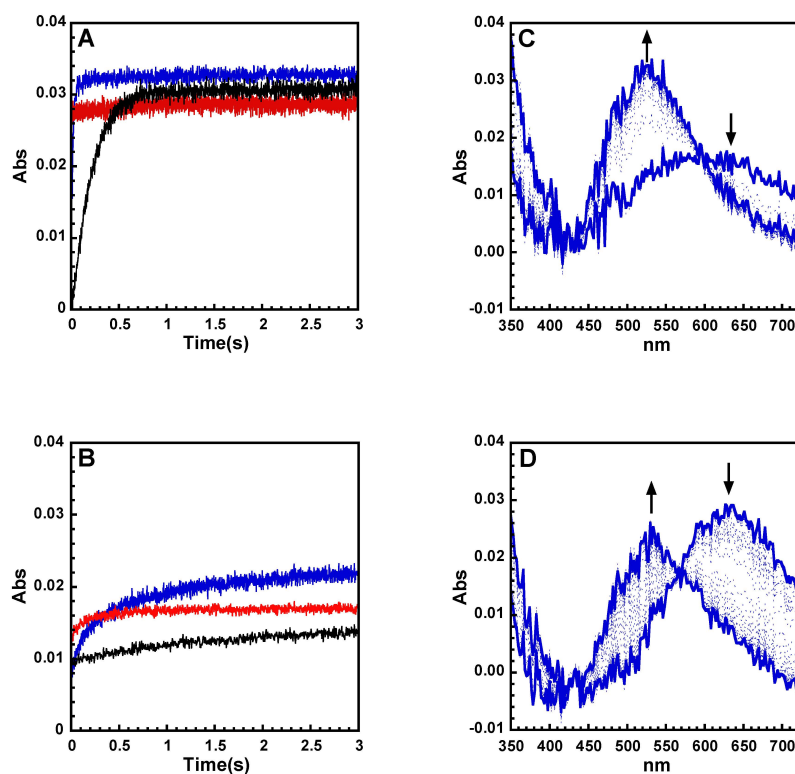
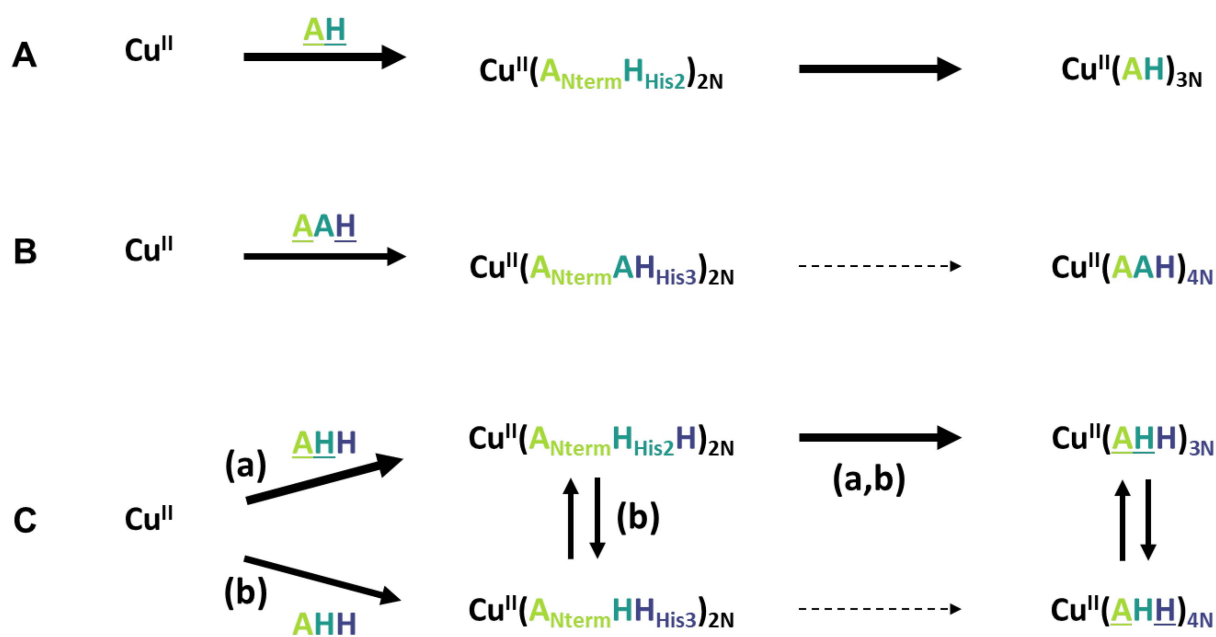


**Figure 3.** Stopped-flow kinetic traces of  $\text{Cu}^{\text{II}}$  coordination by the peptides AH (red), AAH (black), and AHH (blue) (panel (A) ( $\text{Cu}^{\text{II}}$  only); panel (B) ( $\text{Cu}^{\text{II}}$ (A $\beta$ )) and selection of corresponding UV-Vis spectra (panels (C) and (D), respectively). The absorption was measured at 590 nm for AH and at 530 nm for AAH and AHH. Measurements were performed in 100 mM HEPES buffer (pH 7.4) at 25 °C. Final concentrations:  $[\text{Cu}^{\text{II}}] = 450 \mu\text{M}$ ,  $[\text{peptide}] = [\text{A}\beta] = 500 \mu\text{M}$ .



The formation of Cu(AAH) is at least 20 times slower than that of Cu(AH). To account for this difference, we have to take into consideration very recent reports on the kinetics of formation of ATCUN Cu<sup>II</sup> complexes [81–86]. It proceeds via several successive steps: anchoring of the Cu<sup>II</sup> by the imidazole ring of His, then formation of a metallacycle with the anchoring of the N-terminal amine, leading to the 2N intermediate (Scheme S2 for a drawing of the various intermediates described in this work) and rearrangement of the 4N ATCUN motif [81]. The rate-limiting step is the 2N → 4N corresponding to the deprotonation of the peptide bond in between the two anchors. We can thus hypothesize a similar binding pathway for the formation of the Cu(AH) complex, id est, anchoring of the Cu<sup>II</sup> by the imidazole ring of His, then formation of a metallacycle with the anchoring of the N-terminal amine, leading to the 2N intermediate and formation of the 3N motif. In the case of AH, the various rates would be strongly higher than that of AAH because (i) the smaller size of the metallacycle formed is much more favorable to anchor the N-terminal amine and form the 2N intermediates and (ii) there is only one peptide bond to deprotonate (from 2N to 3N, instead of 4N in the case of AAH) (Scheme 2, panels A and B). In the case of AAH, we do observe the very fast formation of the 2N species absorbing near 700 nm (Figure S3, panel C), reminiscent of those thoroughly described in [81], followed by its evolution to the 4N species, which is the rate-limiting step of the whole reaction.



**Scheme 2.** Summary of kinetic data for the Cu<sup>II</sup> binding by AH (A), AAH (B), and AHH (C). The thickness of the arrows mirrors the rate of the reaction (thicker the arrow, faster the reaction is and dotted arrows correspond to the slowest rate). The His (H) residues underlined in (C) correspond to those involved in Cu<sup>II</sup> anchoring.

For the hybrid peptide AHH, the rate of complex formation is in between those of AH and AAH (Figure 3, panel A). As can be seen in Figure 3, panel C, a large absorption band is observed at about 600 nm that forms rapidly (within the dead time of the stopped flow) and that can be attributed to a mixture of 2N and 3N intermediates. Then it evolves, during the rate-limiting step, toward the 4N species with a maximum absorption at 530 nm. The formation of the 2N and/or 3N species is so fast that we cannot distinguish between the two possible pathways (paths a and b in Scheme 2, panel C).

The same experiment was performed in the presence of Aβ. Overall, all the previous rates of Cu(pep) formation are slowed down (Figure 3, panel B and Figure S4). This is in line with (i) the presence of the pre-equilibrium of Cu<sup>II</sup> to Aβ complexation, leading to a strongly reduced concentration of unbound Cu<sup>II</sup> in solution (dissociative path, Scheme S3)

and/or (ii) the more difficult  $\text{Cu}^{\text{II}}$  anchoring when already bound to  $\text{A}\beta$  (associative path). Based on a recent report [82], we propose that the dissociation path is predominant. Such a contribution of the dissociation path is even more pronounced at the concentration of ROS experiments (50 times lower than in the stopped-flow experiments). For AHH,  $\text{Cu}^{\text{II}}$  extraction from  $\text{A}\beta$  is observed concomitantly to the formation of the  $\text{Cu}(\text{AHH})$  complex in its  $4\text{N}$  form detected at a  $\lambda_{\text{max}}$  of 530 nm (Figure 3, panel D) and the formation of the  $\text{Cu}(\text{AHH})_{4\text{N}}$  is about 15 times slower than in the absence of  $\text{A}\beta$ . No intermediate species is detected, as indicated by the presence of the isosbestic point at 560 nm. This is in line with a slowdown of their formation rate (due to a decreased concentration of free  $\text{Cu}^{\text{II}}$  in solution in the presence of  $\text{A}\beta$ ), which thus becomes slower than the conversion to the  $4\text{N}$  species. In the presence of  $\text{A}\beta$ , the formation of the intermediate species thus becomes the rate-limiting step.

### 2.3. Effect of $\text{Zn}^{\text{II}}$ on $\text{Cu}(\text{A}\beta)$ -Induced ROS Production

In a last part, we investigated how  $\text{Zn}^{\text{II}}$  (and other biologically relevant ions) perturb the arrest of  $\text{Cu}(\text{A}\beta)$ -induced ROS production, as  $\text{Zn}^{\text{II}}$  is one of the metal ions whose content is dysregulated in AD. Asc consumption experiments were performed with an increasing amount of  $\text{Zn}^{\text{II}}$  (0 to 10 eq) (Figure 4, Figures S5 and S6). For the three peptides studied here, an increasing amount of  $\text{Zn}^{\text{II}}$  resulted in a slower Asc consumption. This effect was weak in the case of AHH, since the ROS production rate is already slow, but meaningful, since with  $\text{Ca}^{\text{II}}$  and  $\text{Mg}^{\text{II}}$ , no modification is observed (Figure 4). Thus, for the three peptides,  $\text{Zn}^{\text{II}}$  seems to facilitate  $\text{Cu}^{\text{II}}$  binding by the peptides. This is in line with the dissociative pathway we favored previously, where 10 equiv. of  $\text{Zn}^{\text{II}}$  can push  $\text{Cu}^{\text{II}}$  out of the  $\text{A}\beta$  peptide, but not from the AH, AHH, and AAH ones because the  $\text{Zn}^{\text{II}}$  sites are much weaker than that of the  $\text{Cu}^{\text{II}}$ . In other words, based on these results, we proposed a push–pull mechanism in which the  $\text{Zn}^{\text{II}}$  bound to  $\text{A}\beta$  helps to direct  $\text{Cu}^{\text{II}}$  into the AH, AAH, and AHH ligands.

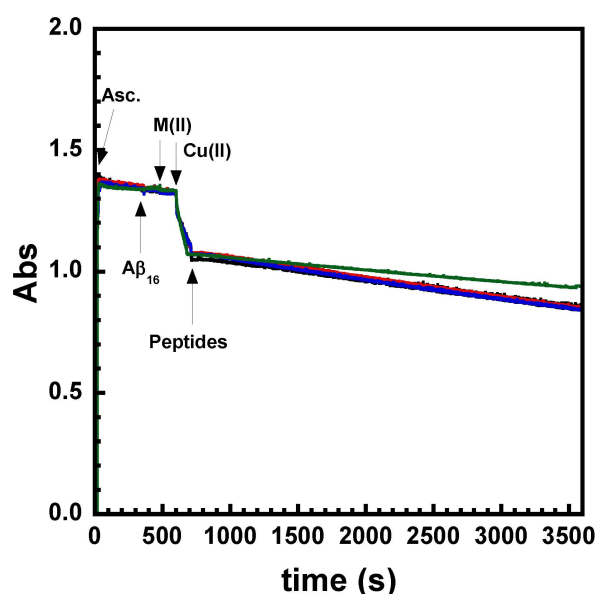
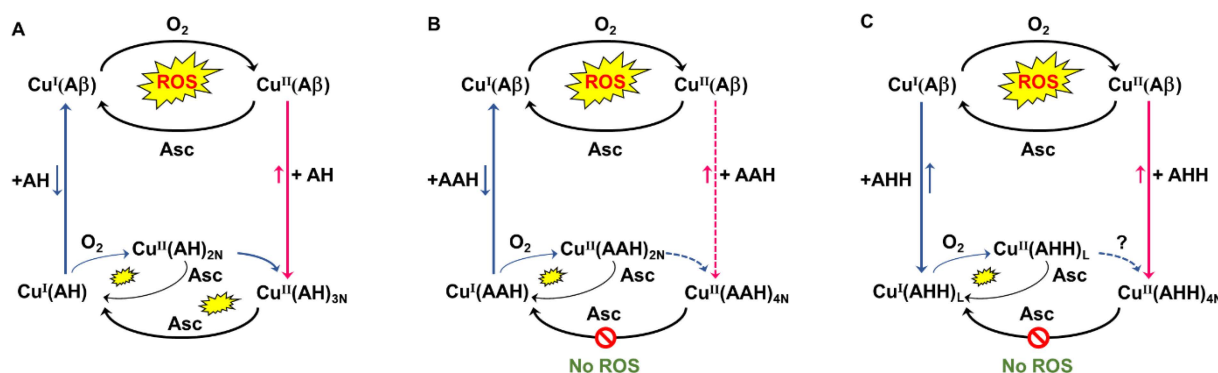


**Figure 4.** Ascorbate consumption (measured at  $\lambda = 265$  nm) as a function of time. Ascorbate was added first, followed by  $\text{A}\beta$  at 6 min,  $\text{Zn}^{\text{II}}$  (green),  $\text{Mg}^{\text{II}}$  (blue),  $\text{Ca}^{\text{II}}$  (red), and no ions (grey) at 10 equiv. versus  $\text{Cu}^{\text{II}}$  at 8 min, and  $\text{Cu}^{\text{II}}$  at 10 min, and, finally, the AHH peptide when an absorbance of 1.2 was reached. Measurements were performed in 50 mM HEPES buffer (pH 7.5) at 25 °C with continuous stirring. Final concentrations:  $[\text{Asc}] = 100 \mu\text{M}$ ,  $[\text{A}\beta] = [\text{peptide}] = 12 \mu\text{M}$ ,  $[\text{Cu}^{\text{II}}] = 10 \mu\text{M}$ ,  $[\text{Zn}^{\text{II}}] = [\text{Ca}^{\text{II}}] = [\text{Mg}^{\text{II}}] = 100 \mu\text{M}$ .



### 3. Concluding Remarks

A tentative picture of the mode of action of the three peptides under focus can thus be drawn (Scheme 3A–C). Addition of peptides during Cu(A $\beta$ )-induced Asc consumption leads to Cu<sup>II</sup> extraction from A $\beta$ . This reaction competes with the reduction of Cu<sup>II</sup>(A $\beta$ ) to Cu<sup>I</sup>(A $\beta$ ) and is fast enough only in the cases of AH and AHH. Once formed, the resulting Cu(AH)<sub>3N</sub> is weakly competent in ROS production, while Cu(AHH)<sub>4N</sub> complexes are resistant to Asc reduction. Only the AHH peptide can both remove Cu<sup>II</sup> from A $\beta$  and form a Cu<sup>II</sup>(AHH) complex resistant to reduction by Asc (and thus is unable to produce ROS). The addition of Zn<sup>II</sup> improves slightly the effect of the peptides due to an increase in the Cu(A $\beta$ ) dissociation pre-equilibrium. This indicates that Zn<sup>II</sup> selectivity of the AHH peptide is, as explained in the introduction, fully appropriate.



**Scheme 3.** Proposed mechanisms by which the Cu(A $\beta$ )-induced ROS production is impacted by the AH (left, panel (A)), AAH (middle, panel (B)), and AHH (right, panel (C)). Dotted lines indicate slow reactions. The size of the star mirrors the level of ROS formed by the redox couple at play.

The presence of two His residues could also give to AHH the additional possibility to compete for Cu<sup>I</sup> with A $\beta$ , leading an L-motif (Scheme 1), while the Cu<sup>I</sup> affinity of AH and AAH, containing only one His, is too weak to do so. After oxidation of Cu<sup>I</sup>, the intermediate formed could either rearrange to form the Cu<sup>II</sup>(AHH)<sub>4N</sub> or be reduced by Asc. To probe the Cu<sup>I</sup> path (blue lines in Scheme 3), the AAHH peptide was tested (Figure S7). This peptide possesses two His residues and is thus able to bind Cu<sup>I</sup> in an L-motif, similarly to AHH, and to compete with A $\beta$  for Cu<sup>I</sup> binding. The results obtained show that AAHH has a weaker ability to arrest Cu(A $\beta$ )-induced ROS formation than AHH. This suggests that the Cu<sup>I</sup> path might not be the one predominant here. We must be very cautious, since two key reactions occurs in the Cu<sup>I</sup> path: (1) Cu<sup>I</sup> extraction from A $\beta$ , which would be similar in case of AHH and AAHH, and (2) the rate of reorganization to the Cu<sup>II</sup>-4N species once the linear Cu<sup>I</sup> intermediate is oxidized, a parameter that could differ between AHH and AAHH (with a fast enough reorganization in case of AHH but not AAHH). To gain further insights into the mechanism at play during ROS production and to discard the Cu<sup>I</sup> path, more systematic studies of the impact of sequence modification (number and position of the His residues) on the level of ROS arrest are needed and are currently under investigation in our group.

In the present study, we have unambiguously shown that the AHH motif is fully appropriate to stop Cu(A $\beta$ )-induced ROS production. AHH combines the two advantageous properties of the two AH and AAH parent ligands, fast Cu<sup>II</sup> binding, and ability to form a redox-incompetent Cu<sup>II</sup> complex, respectively. This result underlines the potential of peptide ligands in the search for Cu-targeting therapeutic approaches in the context of AD. It is also interesting to note that for all the previous ATCUN peptides studied, only experiments where the peptide is added to Cu<sup>II</sup>(A $\beta$ ) and then the ROS production is triggered by addition of Asc have been reported [67–73]. Once formed, Cu<sup>II</sup>(ATCUN) complexes have a very low ability to form ROS, as shown here and previously [55,56,87]. Hence, such studies are incomplete. Indeed, in the brain, which is a quite reductive medium [88,89], with up to

300  $\mu\text{M}$  of Asc being present extracellularly, both redox states of the Cu ions are at play and the Cu(A $\beta$ ) may be redox cycling. Hence, targeting both Cu<sup>I</sup> and Cu<sup>II</sup> ions [90], or having fast enough Cu<sup>II</sup>-complexing agents, are crucial [80,91]. In other words, if ATCUN-based peptides are aimed to be used against Cu(A $\beta$ )-induced ROS formation, the rate of Cu<sup>II</sup> extraction from A $\beta$  matters and, as we demonstrated, such a kinetic parameter is highly dependent on the exact sequence of the ATCUN peptide chosen. It is here interesting to note that, among the N-terminally truncated forms of A $\beta$  recently put forward [92–96], several of them possess such H<sub>2</sub>N-Xxx-His (3N, A $\beta$ <sub>5-x</sub>) [97,98], H<sub>2</sub>N-Xxx-Zzz-His (4N, A $\beta$ <sub>4-x</sub>, [85,86] A $\beta$ <sub>11-x</sub> [86]), and H<sub>2</sub>N-Xxx-His-His (hybrid 3N/4N, A $\beta$ <sub>12-x</sub> [99]) binding sites. Based on our results, the cleavage at position 12 leading to the hybrid 3N/4N binding site may be the most beneficial with respect to Cu(A $\beta$ <sub>1-x</sub>)-induced ROS formation.

Further works will include modifications of the peptide scaffold to obtain BBB penetration and better metabolic stability. This can be straightforward by appending brain-penetrating sequences and using D-peptide, respectively. To shuttle Cu inside cells is also regarded as an interesting additional property that will overcome the intracellular Cu depletion involved in the disability of secretases to clear A $\beta$  [100–102]. This is an exciting follow-up of the present work, which is currently under progress in our team.

## 4. Experimental Section

### 4.1. Chemicals

Reagents were commercially available and were used as received. HEPES buffer (sodium salt of 2-[4-(2-hydroxyethyl)piperazin-1-yl]ethanesulfonic acid) was bought from Fluka (bioluminescence grade).

The Cu<sup>II</sup> and Zn<sup>II</sup> sources were Zn(SO<sub>4</sub>)(H<sub>2</sub>O) and CuCl<sub>2</sub>(H<sub>2</sub>O)<sub>2</sub> and purchased from Sigma. The concentration of Cu<sup>II</sup> was determined by dissolving the Cu salt in Milli-Q water to prepare a 100 mM solution considering an extinction coefficient of  $\epsilon = 12 \text{ M}^{-1} \text{ cm}^{-1}$ . The concentration of Zn<sup>II</sup> was determined by weight.

A stock solution (100 mM) of ascorbate was prepared in Milli-Q water at room temperature just before beginning the experiment.

### 4.2. Peptides

A $\beta$ <sub>1-16</sub> peptide (sequence DAEFRHDSGYEVHHQK, H<sub>2</sub>N-Asp-Ala-Glu-Phe-Arg-His-Asp-Ser-Gly-Tyr-Glu-Cal-His-His-Gln-Lys-COOH, with the three-letter code and referred to as A $\beta$  in the text unless specified, see Scheme 1) was bought from GeneCust (Dudelange, Luxembourg) with a purity grade >98%. Stock solutions of the A $\beta$  peptide were prepared by dissolving the powder in Milli-Q water (resulting pH ~2) at approx. 10 mM. Peptide concentration was then determined by UV-Visible absorption of Tyr10 considered as free tyrosine (at pH 2, ( $\epsilon_{276} - \epsilon_{296}$ ) = 1410 M<sup>-1</sup> cm<sup>-1</sup>). The solutions were diluted down to the appropriate concentration.

### 4.3. Synthesis of Peptides

The AHH, AAH, and AH peptides were synthesized manually with standard 9-fluorenylmethoxycarbonyl (Fmoc) Chemistry on a Fmoc-L-His(Trt)-Wang resin (0.63 mmol/g from Iris Biotech GMBH), through solid-phase peptide synthesis protocols, as previously reported [51].

Stock solutions of peptides were prepared by dissolving the peptides in Milli-Q water. Concentrations were determined by Cu<sup>II</sup> titration followed by UV-Vis absorption spectroscopy.

### 4.4. UV-Visible Spectroscopy

UV-Vis experiments were performed on a Cary-60 UV-Vis spectrometer at 25 °C with constant stirring.

#### 4.5. Ascorbate Consumption Assay

Ascorbate consumption was monitored by UV–Vis. Intensity of the Asc absorption band at  $\lambda = 265$  nm ( $\epsilon = 14\,500$  M<sup>-1</sup> cm<sup>-1</sup>) was monitored as a function of time.

#### 4.6. Stopped-Flow Experiments

Rapid-mixing UV–Vis spectroscopy was carried out using an SFM-20 two-syringe stopped-flow from Biologic combined with a diode array spectrometer composed of a TIDAS J&M MMS-UV/VIS 500-3 detector and a light source HAMAMATSU L7893 light source incorporating a deuterium and a tungsten lamp with optic fibers. Data acquisition, extraction, and treatment were realized with Bio-Kine software. The syringes (Hamilton) were mounted on a rigid drive platform ensuring that the flow was stopped precisely and instantaneously. The contents of the two syringes were rapidly mixed in the mixing chamber and the absorbance of the system recorded over time as full spectra at designated time delays. Typically, one syringe was filled with a solution of peptide at 1 mM in HEPES buffer (200 mM, pH 7.4), and the other one was filled with a solution of CuSO<sub>4</sub> in water at 0.9 mM. An equal quantity of the two solutions were mixed to reach a final concentration of Cu<sup>II</sup> of 450  $\mu$ M and peptide of 500  $\mu$ M in HEPES buffer (100 mM, pH 7.4). The optical length of the UV cuvette is 1 cm.

**Supplementary Materials:** The following supporting information can be downloaded at: <https://www.mdpi.com/article/10.3390/biom12101327/s1>, Figure S1: Ascorbate consumption of Cu<sup>II</sup> and Cu<sup>II</sup>(A $\beta$ ) plus the three AH, AAH and AHH peptides; Figure S2: Ascorbate consumption of Cu<sup>II</sup>(AHH) and Cu<sup>II/I</sup> plus AHH peptide as a function of pH; Figure S3: Stopped-flow kinetic measurements of Cu<sup>II</sup> coordination by AH, AAH and AHH peptides; Figure S4: Stopped-flow kinetic measurements of Cu<sup>II</sup>(A $\beta$ ) capture removal by AH, AAH and AHH peptides; Figure S5: Ascorbate consumption of Cu<sup>II</sup> plus the three AH, AAH and AHH peptides in presence of increasing amounts of Zn<sup>II</sup>; Figure S6: Ascorbate consumption of Cu<sup>II</sup> plus the AH and AAH peptides in presence of various dications; Figure S7: Ascorbate consumption of Cu<sup>II</sup>(A $\beta$ ) plus the four AH, AAH, AHH and AAHH peptides; Scheme S1: Proposed coordination sites in the intermediates 2N forms for the AH, AAH and AHH peptides; Scheme S2: Proposed mechanism corresponding to Cu<sup>II</sup> capture out from A $\beta$  by AH (A), AAH (B) and AHH (C); Scheme S3: Proposed coordination sites in the ternary species obtained upon AH and AHH addition to Cu<sup>II</sup>(A $\beta$ ) [60,62,82].

**Author Contributions:** Conceptualization, C.H.; formal analysis, P.G., E.M., L.S., P.F., C.H.; investigation, P.G. and L.S.; data curation, L.S. and E.M.; writing—original draft preparation, P.G., E.M. and C.H.; writing—review and editing, C.H.; supervision, P.F. and C.H.; project administration, C.H.; funding acquisition, C.H. All authors have read and agreed to the published version of the manuscript.

**Funding:** ERC aLzINK-StG 638712 (attributed to C.H.) is acknowledged for funding.

**Institutional Review Board Statement:** Not applicable.

**Informed Consent Statement:** Not applicable.

**Data Availability Statement:** Not applicable.

**Acknowledgments:** C. Esmieu is acknowledged for fruitful discussions. C.H., L.S., P.G., P.F. thank ERC aLzINK-StG 638712 (attributed to C.H.) for funding.

**Conflicts of Interest:** The authors declare no conflict of interest.

## References

1. Available online: <https://www.alzint.org/about/dementia-facts-figures/dementia-statistics/> (accessed on 18 August 2022).
2. Available online: <https://www.brightfocus.org/alzheimers/article/alzheimers-disease-facts-figures> (accessed on 18 August 2022).
3. Available online: [https://aaic.alz.org/releases\\_2021/global-prevalence.asp](https://aaic.alz.org/releases_2021/global-prevalence.asp) (accessed on 18 August 2022).
4. Available online: <https://www.who.int/news-room/fact-sheets/detail/dementia> (accessed on 18 August 2022).
5. Hampel, H.; Hardy, J.; Blennow, K.; Chen, C.; Perry, G.; Kim, S.H.; Vilmagne, V.L.; Aisen, P.; Vendruscolo, M.; Iwatsubo, T.; et al. The Amyloid- $\beta$  Pathway in Alzheimer's Disease. *Mol. Psychiatry* **2021**, *26*, 5481–5503. [CrossRef] [PubMed]
6. Padhi, D.; Govindaraju, T.J. Mechanistic Insights for Drug Repurposing and the Design of Hybrid Drugs for Alzheimer's Disease. *Med. Chem.* **2022**, *65*, 7088–7105. [CrossRef] [PubMed]

7. Gong, C.X.; Dai, C.L.; Liu, F.; Iqbal, K. Multi-Targets: An Unconventional Drug Development Strategy for Alzheimer's Disease. *Front. Aging Neurosci.* **2022**, *14*, 837649. [[CrossRef](#)] [[PubMed](#)]
8. Cummings, J.; Lee, G.; Nahed, P.; Kamar, M.E.Z.N.; Zhong, K.; Fonseca, J.; Taghva, K. Alzheimer's disease drug development pipeline: 2022. *Alzheimer's Dement. Transl. Res. Clin. Interv.* **2022**, *8*, e12295. [[CrossRef](#)] [[PubMed](#)]
9. Athar, T.; Al Balushi, K.; Khan, S.A. Challenges of peptide and protein drug delivery by oral route: Current strategies to improve the bioavailability. *Mol. Biol. Rep.* **2021**, *48*, 5629–5645. [[CrossRef](#)] [[PubMed](#)]
10. Liu, Y.; Cong, L.; Han, C.; Li, B.; Dai, R. Recent Progress in the Drug Development for the Treatment of Alzheimer's Disease Especially on Inhibition of Amyloid-peptide Aggregation. *Mini-Rev. Med. Chem.* **2021**, *21*, 969–990. [[CrossRef](#)] [[PubMed](#)]
11. Priya, K.; Siddesha, J.M.; Dharini, S.; Shashanka, K.P. Interacting Models of Amyloid- $\beta$  and Tau Proteins: An Approach to Identify Drug Targets in Alzheimer's Disease. *J. Alzheimer's Dis. Rep.* **2021**, *5*, 405–411. [[CrossRef](#)] [[PubMed](#)]
12. West, S.; Bhugra, P. Emerging drug targets for A $\beta$  and tau in Alzheimer's disease: A systematic review. *Br. J. Clin. Pharmacol.* **2015**, *80*, 221–234. [[CrossRef](#)]
13. Singh, S.K.; Balendra, V.; Obaid, A.A.; Esposto, J.; Tikhonova, M.A.; Gautam, N.K.; Poeggeler, B. Copper-mediated  $\beta$ -amyloid toxicity and its chelation therapy in Alzheimer's disease. *Metallomics* **2022**, *14*, mfac018. [[CrossRef](#)]
14. Fasae, K.D.; Abolaji, A.O.; Faloye, T.R.; Odunsi, A.Y.; Oyeyayo, B.O.; Enya, J.I.; Rotimi, J.A.; Akinyemi, R.O.; Whitworth, A.J.; Aschner, M.J. Metallobiology and therapeutic chelation of biometals (copper, zinc and iron) in Alzheimer's disease: Limitations, and current and future perspectives. *Trace Elem. Med. Biol.* **2021**, *67*, 126779. [[CrossRef](#)]
15. Ejaz, H.W.; Wang, W.; Lang, M. Copper toxicity links to pathogenesis of Alzheimer's disease and therapeutics approaches. *Int. J. Mol. Sci.* **2020**, *21*, 7660. [[CrossRef](#)]
16. Esmieu, C.; Guettas, D.; Conte-Daban, A.; Sabater, L.; Faller, P.; Hureau, C. Copper-Targeting Approaches in Alzheimer's Disease: How To Improve the Fallouts Obtained from in Vitro Studies. *Inorg. Chem.* **2019**, *58*, 13509–13527. [[CrossRef](#)]
17. Savelieff, M.G.; Nam, G.; Kang, J.; Lee, H.J.; Lee, M.; Lim, M.H. Development of Multifunctional Molecules as Potential Therapeutic Candidates for Alzheimer's Disease, Parkinson's Disease, and Amyotrophic Lateral Sclerosis in the Last Decade. *Chem. Rev.* **2019**, *119*, 1221–1322. [[CrossRef](#)]
18. Robert, A.; Liu, Y.; Nguyen, M.; Meunier, B. Regulation of copper and iron homeostasis by metal chelators: A possible chemotherapy for Alzheimer's disease. *Acc. Chem. Res.* **2015**, *48*, 1332–1339. [[CrossRef](#)]
19. Weibull, M.G.M.; Simonsen, S.; Oksbjerg, C.R.; Tiwari, M.K.; Hemmingsen, L. Effects of Cu(II) on the aggregation of amyloid- $\beta$ . *J. Biol. Inorg. Chem.* **2019**, *24*, 1197–1215. [[CrossRef](#)]
20. Cheignon, C.; Tomas, M.; Bonnefont-Rousselot, D.; Faller, P.; Hureau, C.; Collin, F. Oxidative stress and the amyloid beta peptide in Alzheimer's Disease. *Redox Biol.* **2018**, *14*, 450–464. [[CrossRef](#)]
21. Huat, T.J.; Camats-Perna, J.; Newcombe, E.A.; Valmas, N.; Kitazawa, M.; Medeiros, R.J. Metal Toxicity Links to Alzheimer's Disease and Neuroinflammation. *Mol. Biol.* **2019**, *431*, 1843–1868. [[CrossRef](#)]
22. Reybier, K.; Ayala, S.; Alies, B.; Bustos Rodriguez, S.; Rodrigues, J.; Gomes, C.; La Penna, G.; Collin, F.; Hureau, C.; Faller, P. Free superoxide is an intermediate in the production of H<sub>2</sub>O<sub>2</sub> by Cu(I)-amyloid- $\beta$  and O<sub>2</sub>. *Angew. Chem. Int. Ed.* **2016**, *55*, 1085–1089. [[CrossRef](#)]
23. Nandi, A.; Yan, L.J.; Jana, C.K.; Das, N. Role of Catalase in Oxidative Stress- and Age-Associated Degenerative Diseases. *Oxidative Med. Cell. Longev.* **2019**, *2019*, 9613090. [[CrossRef](#)]
24. Guilloreau, L.; Combalbert, S.; Sournia-Saquet, A.; Marzaguil, H.; Faller, P. Redox Chemistry of Copper-Amyloid-beta: The Generation of Hydroxyl Radical in the Presence of Ascorbate is Linked to Redox-Potentials and Aggregation State. *ChemBioChem* **2007**, *8*, 1317–1325. [[CrossRef](#)]
25. Dikalov, S.I.; Vitek, M.P.; Mason, R.P. Cupric-amyloid beta peptide complex stimulates oxidation of ascorbate and generation of hydroxyl radical. *Free Radic. Biol. Med.* **2004**, *36*, 340–347. [[CrossRef](#)]
26. Bellotti, D.; Remelli, M. Lights and Shadows on the Therapeutic Use of Antimicrobial Peptides. *Molecules* **2022**, *27*, 4584. [[CrossRef](#)]
27. Li Petri, G.; Di Martino, S.; De Rosa, M.J. Peptidomimetics: An Overview of Recent Medicinal Chemistry Efforts toward the Discovery of Novel Small Molecule Inhibitors. *Med. Chem.* **2022**, *65*, 7438–7475. [[CrossRef](#)]
28. Lai, X.; Tang, J.; ElSayed, M.E.H. Recent advances in proteolytic stability for peptide, protein, and antibody drug discovery. *Exp. Opin. Drug Discov.* **2021**, *16*, 1467–1482. [[CrossRef](#)]
29. Wątyły, J.; Miller, A.; Kozłowski, H.; Rowińska-Żyrek, M.J. Peptidomimetics – An infinite reservoir of metal binding motifs in metabolically stable and biologically active molecules. *Inorg. Biochem.* **2021**, *217*, 111386. [[CrossRef](#)]
30. Aileen Funke, S.; van Groen, T.; Kadish, I.; Bartnik, D.; Nagel-Steger, L.; Brener, O.; Sehl, T.; Batra-Safferling, R.; Moriscot, C.; Schoehn, G.; et al. Oral treatment with the d-enantiomeric peptide D3 improves the pathology and behavior of Alzheimer's Disease transgenic mice. *ACS Chem. Neurosci.* **2010**, *1*, 639–648. [[CrossRef](#)]
31. Verma, S.; Goand, U.K.; Husain, A.; Katekar, R.A.; Garg, R.; Gayen, J.R. Challenges of peptide and protein drug delivery by oral route: Current strategies to improve the bioavailability. *Drug Dev. Res.* **2021**, *82*, 927–944. [[CrossRef](#)]
32. Covarrubias-Zambrano, O.; Yu, J.; Bossmann, H.S. Nano-Inspired Technologies for Peptide Delivery. *Curr. Protein Pept. Sci.* **2020**, *21*, 379–400. [[CrossRef](#)]
33. Makowski, M.; Silva, Í.C.; Pais do Amaral, C.; Gonçalves, S.; Santos, N.C. Advances in lipid and metal nanoparticles for antimicrobial peptide delivery. *Pharmaceutics* **2019**, *11*, 588. [[CrossRef](#)]



34. Tang, Y.; Varyambath, A.; Ding, Y.; Chen, B.; Huang, X.; Zhang, Y.; Yu, D.-g.; Kim, I.; Song, W. Porous organic polymers for drug delivery: Hierarchical pore structures, variable morphologies, and biological properties. *Biomater. Sci.* **2022**. [[CrossRef](#)]
35. Reissmann, S.; Filatova, M.P. New generation of cell-penetrating peptides: Functionality and potential clinical application. *J. Pept. Sci.* **2021**, *27*, e3300. [[CrossRef](#)] [[PubMed](#)]
36. Zhou, X.; Smith, Q.R.; Liu, X. Brain penetrating peptides and peptide–drug conjugates to overcome the blood–brain barrier and target CNS diseases. *WIREs Nanomed. Nanobiotechnology* **2021**, *13*, e1695. [[CrossRef](#)] [[PubMed](#)]
37. Zhang, Y.; Kim, I.; Lu, Y.; Xu, Y.; Yu, D.-G.; Song, W. Intelligent poly(L-histidine)-based nanovehicles for controlled drug delivery. *J. Control. Release* **2022**, *349*, 963–982. [[CrossRef](#)] [[PubMed](#)]
38. Zhang, Y.; Song, W.; Lu, Y.; Xu, Y.; Wang, C.; Yu, D.-G.; Kim, I. Recent Advances in Poly(L-glutamic acid)-Based Nanomaterials for Drug Delivery. *Biomolecules* **2022**, *12*, 636. [[CrossRef](#)]
39. Atrian-Blasco, E.; Conte-Daban, A.; Hureau, C. Mutual interference of Cu and Zn ions in Alzheimer’s disease: Perspectives at the molecular level. *Dalton Trans.* **2017**, *46*, 12750–12759. [[CrossRef](#)]
40. Atrian-Blasco, E.; Gonzalez, P.; Santoro, A.; Alies, B.; Faller, P.; Hureau, C. Cu and Zn coordination to amyloid peptides: From fascinating chemistry to debated pathological relevance. *Coord. Chem. Rev.* **2018**, *375*, 38–55. [[CrossRef](#)]
41. Rana, M.; Sharma, A.K. Cu and Zn interactions with A $\beta$  peptides: Consequence of coordination on aggregation and formation of neurotoxic soluble A $\beta$  oligomers. *Metallomics* **2019**, *11*, 64–84. [[CrossRef](#)]
42. Dorlet, P.; Gambarelli, S.; Faller, P.; Hureau, C. Pulse EPR Spectroscopy Reveals the Coordination Sphere of Copper(II) Ions in the 1–16 Amyloid- $\beta$  Peptide: A Key Role of the First Two N-Terminus Residues. *Angew. Chem. Int. Ed. Engl.* **2009**, *48*, 9273–9276. [[CrossRef](#)]
43. Alies, B.; Conte-Daban, A.; Sayen, S.; Collin, F.; Kieffer, I.; Guillon, E.; Faller, P.; Hureau, C. Zinc(II) Binding Site to the Amyloid- $\beta$  Peptide: Insights from Spectroscopic Studies with a Wide Series of Modified Peptides. *Inorg. Chem.* **2016**, *55*, 10499–10509. [[CrossRef](#)]
44. De Gregorio, G.; Biasotto, F.; Hecel, A.; Luczkowski, M.; Kozłowski, H.; Valensin, D. Structural analysis of copper(I) interaction with amyloid  $\beta$  peptide. *J. Inorg. Biochem.* **2019**, *195*, 31–38. [[CrossRef](#)]
45. Hureau, C.; Balland, V.; Coppel, Y.; Solari, P.L.; Fonda, E.; Faller, P. Importance of dynamical processes in the coordination chemistry and redox conversion of copper amyloid- $\beta$  complexes. *J. Biol. Inorg. Chem.* **2009**, *14*, 995–1000. [[CrossRef](#)]
46. Alies, B.; Renaglia, E.; Rozga, M.; Bal, W.; Faller, P.; Hureau, C. Cu(II) affinity for the Alzheimer’s Peptide: Tyrosine fluorescence studies revisited. *Anal. Chem.* **2013**, *85*, 1501–1508. [[CrossRef](#)]
47. Zawisza, I.; Rozga, M.; Bal, W. Affinity of peptides (A $\beta$ , APP,  $\alpha$ -synuclein, PrP) for metal ions (Cu, Zn). *Coord. Chem. Rev.* **2012**, *256*, 2297–2307. [[CrossRef](#)]
48. Alies, B.; Badei, B.; Faller, P.; Hureau, C. Reevaluation of Copper(I) affinity for amyloid- $\beta$  peptides by competition with Ferrozine—An unusual Copper(I) indicator. *Chem. Eur. J.* **2012**, *18*, 1161–1167. [[CrossRef](#)]
49. Young, T.R.; Kirchner, A.; Wedd, A.G.; Xiao, Z. An integrated study of the affinities of the A $\beta$ 16 peptide for Cu(I) and Cu(II): Implications for the catalytic production of reactive oxygen species. *Metallomics* **2014**, *6*, 505–517. [[CrossRef](#)]
50. Xiao, Z.; Gottschlich, L.; van der Meulen, R.; Udagedara, S.R.; Wedd, A.G. Evaluation of quantitative probes for weaker Cu(i) binding sites completes a set of four capable of detecting Cu(I) affinities from nanomolar to attomolar. *Metallomics* **2013**, *5*, 501–513. [[CrossRef](#)]
51. Gonzalez, P.; Vileno, B.; Bossak, K.; El Khoury, Y.; Hellwig, P.; Bal, W.; Hureau, C.; Faller, P. Cu(II)-binding to the peptide Ala-His-His, a chimera of the canonical Cu(II)-binding motifs Xxx-His and Xxx-Zzz-His (ATCUN). *Inorg. Chem.* **2017**, *56*, 14870–14879. [[CrossRef](#)]
52. Pickart, L.; Margolina, A. Regenerative and protective actions of the GHK-Cu peptide in the light of the new gene data. *Int J. Mol. Sci.* **2018**, *19*, 1987. [[CrossRef](#)]
53. Ma, W.H.; Li, M.; Ma, H.F.; Li, W.; Liu, L.; Yin, Y.; Zhou, X.M.; Hou, G. Protective effects of GHK-Cu in bleomycin-induced pulmonary fibrosis via anti-oxidative stress and anti-inflammation pathways. *Life Sci.* **2020**, *241*, 117139. [[CrossRef](#)]
54. Wang, X.; Liu, B.; Xu, Q.; Sun, H.; Shi, M.; Wang, D.; Guo, M.; Yu, J.; Zhao, C.; Feng, B. GHK-Cu-liposomes accelerate scald wound healing in mice by promoting cell proliferation and angiogenesis. *Wound Repair Regen.* **2017**, *25*, 270–278. [[CrossRef](#)]
55. Hureau, C.; Eury, H.; Guillot, R.; Bijani, C.; Sayen, S.; Solari, P.L.; Guillon, E.; Faller, P.; Dorlet, P. X-Ray and solution structures of CuGHK and CuDAHK complexes. Influence on their redox properties. *Chem. Eur. J.* **2011**, *17*, 10151–10160. [[CrossRef](#)]
56. Gonzalez, P.; Bossak, K.; Stefaniak, E.; Hureau, C.; Raibaut, L.; Bal, W.; Faller, P. N-terminal Cu Binding Motifs Xxx-Zzz-His (ATCUN) and Xxx-His and their derivatives: Chemistry, Biology and Medicinal Applications. *Chem. Eur. J.* **2018**, *24*, 8029–8041. [[CrossRef](#)]
57. Maiti, B.K.; Govil, N.; Kundu, T.; Moura, J.J.G. Designed Metal-ATCUN Derivatives: Redox- and Non-redox-Based Applications Relevant for Chemistry, Biology, and Medicine. *iScience* **2020**, *23*, 101792. [[CrossRef](#)]
58. Harford, C.; Sarkar, B. Amino Terminal Cu(II)- and Ni(II)-Binding (ATCUN) Motif of Proteins and Peptides: MetalBinding, DNA Cleavage, and Other Properties. *Acc. Chem. Res.* **1997**, *30*, 123–130. [[CrossRef](#)]
59. Bal, W.; Sokołowska, M.; Kurowska, E.; Faller, P. Binding of transition metal ions to albumin: Sites, affinities and rates. *Biochim. Biophys. Acta* **2013**, *1830*, 5444–5455. [[CrossRef](#)]
60. Gonzalez, P.; Bossak-Ahmad, K.; Vileno, B.; Wezynfeld, N.E.; El Khoury, Y.; Hellwig, P.; Hureau, C.; Bal, W.; Faller, P. Triggering Cu-coordination change in Cu(ii)-Ala-His-His by external ligands. *Chem. Commun.* **2019**, *55*, 8110–8113. [[CrossRef](#)]

61. Trapaidze, A.; Hureau, C.; Bal, W.; Winterhalter, M.; Faller, P. Thermodynamic study of Cu<sup>2+</sup> binding to the DAHK and GHK peptides by isothermal titration calorimetry (ITC) with the weaker competitor glycine. *J. Biol. Inorg. Chem.* **2012**, *17*, 37–47. [[CrossRef](#)]
62. Bossak-Ahmad, K.; Wiśniewska, M.D.; Bal, W.; Drew, S.C.; Frączyk, T. Ternary Cu(II) Complex with GHK Peptide and Cis-Urocanic Acid as a Potential Physiologically Functional Copper Chelate. *Int. J. Mol. Sci.* **2020**, *21*, 6190. [[CrossRef](#)]
63. Sóvágó, I.; Kállay, C.; Várnagy, K. Peptides as complexing agents. Factors influencing the structure and thermodynamic stability of peptide complexes. *Coord. Chem. Rev.* **2012**, *256*, 2225–2233. [[CrossRef](#)]
64. Hureau, C. Coordination of redox active metal ions to the APP and to the amyloid- $\beta$  peptides involved in AD. Part 1: An overview. *Coord. Chem. Rev.* **2012**, *256*, 2164–2174. [[CrossRef](#)]
65. Portelinha, J.; Duay, S.S.; Yu, S.I.; Heilemann, K.; Libardo, M.D.J.; Juliano, S.A.; Klassen, J.L.; Angeles-Boza, A.M. Antimicrobial Peptides and Copper(II) Ions: Novel Therapeutic Opportunities. *Chem. Rev.* **2021**, *121*, 2648–2712. [[CrossRef](#)] [[PubMed](#)]
66. Agbale, C.M.; Cardoso, M.H.; Galyuon, I.K.; Franco, O.L. Designing metallodrugs with nuclease and protease activity. *Metallomics* **2016**, *8*, 1159–1169. [[CrossRef](#)] [[PubMed](#)]
67. Folk, D.S.; Franz, K.J. A prochelator activated by beta-secretase inhibits A $\beta$  aggregation and suppresses copper-induced reactive oxygen species formation. *J. Am. Chem. Soc.* **2010**, *132*, 4994–4995. [[CrossRef](#)] [[PubMed](#)]
68. Caballero, A.B.; Terol-Ordaz, L.; Espargaró, A.; Vázquez, G.; Nicolás, E.; Sabaté, R.; Gamez, P. Histidine-Rich Oligopeptides To Lessen Copper-Mediated Amyloid- $\beta$  Toxicity. *Chem. Eur. J.* **2016**, *22*, 7268–7280. [[CrossRef](#)]
69. Jensen, M.; Canning, A.; Chiha, S.; Bouquerel, P.; Pedersen, J.T.; Østergaard, J.; Cuvillier, O.; Sasaki, I.; Hureau, C.; Faller, P. Bi-functional peptide with  $\beta$ -sheet breaker and chelator moieties against Cu- amyloid- $\beta$ . *Chem. Eur. J.* **2012**, *18*, 4836–4839. [[CrossRef](#)]
70. Hu, X.; Zhang, Q.; Wang, W.; Yuan, Z.; Zhu, X.; Chen, B.; Chen, X. Tripeptide GGH as the Inhibitor of Copper-Amyloid- $\beta$ -Mediated Redox Reaction and Toxicity. *ACS Chem. Neurosci.* **2016**, *7*, 1255–1263. [[CrossRef](#)]
71. Meng, J.; Zhang, H.; Dong, X.; Liu, F.; Sun, Y. RTHLVFFARK-NH<sub>2</sub>: A potent and selective modulator on Cu<sup>2+</sup>-mediated amyloid- $\beta$  protein aggregation and cytotoxicity. *J. Inorg. Biochem.* **2018**, *181*, 56–64. [[CrossRef](#)]
72. Perrone, L.; Mothes, E.; Vignes, M.; Mockel, A.; Figueroa, C.; Miquel, M.C.; Maddelein, M.L.; Faller, P. Copper transfer from Cu-Abeta to human serum albumin inhibits aggregation, radical production and reduces A $\beta$  toxicity. *ChemBioChem* **2010**, *11*, 110–118. [[CrossRef](#)]
73. Mital, M.; Wezynfeld, N.E.; Frączyk, T.; Wiloch, M.Z.; Wawrzyniak, U.E.; Bonna, A.; Tumpach, C.; Barnham, K.J.; Haigh, C.L.; Bal, W.; et al. A Functional Role for A $\beta$  in Metal Homeostasis? N-Truncation and High-Affinity Copper Binding. *Angew. Chem. Int. Ed.* **2015**, *54*, 10460–10464. [[CrossRef](#)]
74. Pushie, M.J.; Stefaniak, E.; Sendzik, M.R.; Sokaras, D.; Kroll, T.; Haas, K.L. Using N-Terminal Coordination of Cu(II) and Ni(II) to Isolate the Coordination Environment of Cu(I) and Cu(II) Bound to His13 and His14 in Amyloid- $\beta$ (4–16). *Inorg. Chem.* **2019**, *58*, 15138–15154. [[CrossRef](#)]
75. Streltsov, V.A.; Ekanayake, R.S.K.; Drew, S.C.; Chantler, C.T.; Best, S.P. Structural Insight into Redox Dynamics of Copper Bound N-Truncated Amyloid- $\beta$  Peptides from In Situ X-ray Absorption Spectroscopy. *Inorg. Chem.* **2018**, *57*, 11422–11435. [[CrossRef](#)]
76. Alies, B.; Sasaki, I.; Proux, O.; Sayen, S.; Guillon, E.; Faller, P.; Hureau, C. Zn impacts Cu coordination to Amyloid- $\beta$ , the Alzheimer's peptide, but not the ROS production and the associated cell toxicity. *Chem. Commun.* **2013**, *49*, 1214–1216. [[CrossRef](#)]
77. Cheignon, C.; Collin, F.; Faller, P.; Hureau, C. Is ascorbate Dr Jekyll or Mr Hyde in the Cu(A $\beta$ ) mediated oxidative stress linked to Alzheimer's Disease? *Dalton Trans.* **2016**, *45*, 12627–12631. [[CrossRef](#)]
78. Chassaing, S.; Collin, F.; Dorlet, P.; Gout, J.; Hureau, C.; Faller, P. Copper and heme-mediated A $\beta$  toxicity: Redox chemistry, Abeta oxidations and anti-ROS compounds. *Curr. Top. Med. Chem.* **2012**, *12*, 2573–2595. [[CrossRef](#)]
79. Conte-Daban, A.; Day, A.; Faller, P.; Hureau, C. How Zn can impede Cu detoxification by chelating agents in Alzheimer's disease: A proof-of-concept study. *Dalton Trans.* **2016**, *45*, 15671–15678. [[CrossRef](#)]
80. Conte-Daban, A.; Beyler, M.; Tripier, R.; Hureau, C. Kinetic is crucial when targeting copper ions to fight Alzheimer's disease: An illustration with azamacrocyclic ligands. *Chem. Eur. J.* **2018**, *24*, 8447–8452. [[CrossRef](#)]
81. Kotuniak, R.; Strampraad, M.J.F.; Bossak-Ahmad, K.; Wawrzyniak, U.E.; Ufnalska, I.; Hagedoorn, P.-L.; Bal, W. Key Intermediate Species Reveal the Copper(II)-Exchange Pathway in Biorelevant ATCUN/NTS Complexes. *Angew. Chem. Int. Ed.* **2020**, *59*, 11234–11239. [[CrossRef](#)]
82. Beuning, C.N.; Zocchi, L.J.; Malikidogo, K.P.; Esmieu, C.; Dorlet, P.; Crans, D.C.; Hureau, C. Measurement of Interpeptidic CuII Exchange Rate Constants of CuII-Amyloid- $\beta$  Complexes to Small Peptide Motifs by Tryptophan Fluorescence Quenching. *Inorg. Chem.* **2021**, *60*, 7650–7659. [[CrossRef](#)]
83. Beuning, C.N.; Mestre-Voegtlé, B.; Faller, P.; Hureau, C.; Crans, D.C. Measurement of Interpeptidic Cu(II) Exchange Rate Constants by Static Fluorescence Quenching of Tryptophan. *Inorg. Chem.* **2018**, *57*, 4791–4794. [[CrossRef](#)]
84. Kotuniak, R.; Bal, W. Kinetics of Cu(ii) complexation by ATCUN/NTS and related peptides: A gold mine of novel ideas for copper biology. *Dalton Trans.* **2022**, *51*, 14–26. [[CrossRef](#)]
85. Teng, X.; Stefaniak, E.; Girvan, P.; Kotuniak, R.; Płonka, D.; Bal, W.; Ying, L. Hierarchical binding of copperII to N-truncated A $\beta$ 4–16 peptide. *Metallomics* **2020**, *12*, 470–473. [[CrossRef](#)]
86. Esmieu, C.; Ferrand, G.; Borghesani, V.; Hureau, C. Impact of N-Truncated A $\beta$  Peptides on Cu- and Cu(A $\beta$ )-Generated ROS: Cu(I) Matters! *Chem. A Eur. J.* **2021**, *27*, 1777–1786. [[CrossRef](#)]



87. Santoro, A.; Walke, G.; Vileno, B.; Kulkarni, P.P.; Raibaut, L.; Faller, P. Low catalytic activity of the Cu(II)-binding motif (Xxx-Zzz-His; ATCUN) in reactive oxygen species production and inhibition by the Cu(I)-chelator BCS. *Chem. Commun.* **2018**, *54*, 11945–11948. [[CrossRef](#)]
88. Harrison, F.E.; May, J.M. Vitamin C function in the brain: Vital role of the ascorbate transporter SVCT2. *Free Radic. Biol. Med.* **2009**, *46*, 719–730. [[CrossRef](#)]
89. Rice, M.E. Ascorbate regulation and its neuroprotective role in the brain. *Trends Neurosci.* **2000**, *23*, 209–216. [[CrossRef](#)]
90. Conte-Daban, A.; Boff, B.; Candido Matias, A.; Montes Aparicio, C.N.; Gateau, C.; Lebrun, C.; Cerchiaro, G.; Kieffer, I.; Sayen, S.; Guillon, E.; et al. A trishistidine pseudopeptide with ability to remove both Cu(I) and Cu(II) from the Alzheimer's peptide and to stop the associated ROS formation. *Chem. Eur. J.* **2017**, *23*, 17078–17088. [[CrossRef](#)]
91. Conte-Daban, A.; Beyler, M.; Tripier, R.; Hureau, C. Corrigendum: Kinetics Are Crucial When Targeting Copper Ions to Fight Alzheimer's Disease: An Illustration with Azamacrocyclic Ligands. *Chem. Eur. J.* **2018**, *24*, 13058. [[CrossRef](#)]
92. Stefaniak, E.; Bal, W. Cu(II) Binding Properties of N-Truncated A $\beta$  Peptides: In Search of Biological Function. *Inorg. Chem.* **2019**, *58*, 13561–13577. [[CrossRef](#)]
93. Rostagno, A.; Cabrera, E.; Lashley, T.; Ghiso, J. N-terminally truncated A $\beta$ 4-x proteoforms and their relevance for Alzheimer's pathophysiology. *Transl. Neurodegener.* **2022**, *11*, 30. [[CrossRef](#)]
94. Borghesani, V.; Alies, B.; Hureau, C. Cu(II) binding to various forms of amyloid- $\beta$  peptides. Are they friends or foes? *Eur. J. Inorg. Chem.* **2018**, 7–15. [[CrossRef](#)]
95. Domingo, G.; Benussi, L.; Saraceno, C.; Bertuzzi, M.; Nicsanu, R.; Longobardi, A.; Bellini, S.; Cagnotto, A.; Salmona, M.; Binetti, G.; et al. N-Terminally Truncated and Pyroglutamate-Modified A $\beta$  Forms Are Measurable in Human Cerebrospinal Fluid and Are Potential Markers of Disease Progression in Alzheimer's Disease. *Front. Neurosci.* **2021**, *15*. [[CrossRef](#)] [[PubMed](#)]
96. Fraczyk, T.; Cieplak, P. Neglected N-Truncated Amyloid- $\beta$  Peptide and Its Mixed Cu–Zn Complexes. *Protein J.* **2022**, *41*, 361–368. [[CrossRef](#)] [[PubMed](#)]
97. Wezynfeld, N.E.; Tobolska, A.; Mital, M.; Wawrzyniak, U.E.; Wiloch, M.Z.; Płonka, D.; Bossak-Ahmad, K.; Wróblewski, W.; Bal, W. A $\beta$ 5-x Peptides: N-Terminal Truncation Yields Tunable Cu(II) Complexes. *Inorg. Chem.* **2020**, *59*, 14000–14011. [[CrossRef](#)] [[PubMed](#)]
98. Tobolska, A.; Wezynfeld, N.E.; Wawrzyniak, U.E.; Bal, W.; Wróblewski, W. Copper(II) complex of N-truncated amyloid- $\beta$  peptide bearing a His-2 motif as a potential receptor for phosphate anions. *Dalton Trans.* **2021**, *50*, 2726–2730. [[CrossRef](#)]
99. Bossak-Ahmad, K.; Mital, M.; Płonka, D.; Drew, S.C.; Bal, W. Oligopeptides Generated by Neprilysin Degradation of  $\beta$ -Amyloid Have the Highest Cu(II) Affinity in the Whole A $\beta$  Family. *Inorg. Chem.* **2019**, *58*, 932–943. [[CrossRef](#)]
100. Crouch, P.J.; Barnham, K.J. Therapeutic redistribution of metal ions to treat Alzheimer's disease. *Acc. Chem. Res.* **2012**, *45*, 1604–1611. [[CrossRef](#)]
101. Crouch, P.J.; Savva, M.S.; Hung, L.W.; Donnelly, P.S.; Mot, A.I.; Parker, S.J.; Greenough, M.A.; Volitakis, I.; Adlard, P.A.; Cherny, R.A.; et al. The Alzheimer's therapeutic PBT2 promotes amyloid- $\beta$  degradation and GSK3 phosphorylation via a metal chaperone activity. *J. Neurochem.* **2011**, *119*, 220–230. [[CrossRef](#)]
102. Filiz, G.; Price, K.A.; Caragounis, A.; Du, T.; Crouch, P.J.; White, A.R. The role of metals in modulating metalloprotease activity in the AD brain. *Eur. Biophys. J.* **2008**, *37*, 315–321. [[CrossRef](#)]